

Investigation of magnetic properties of samarium by the muon method

I. I. Gurevich, I. G. Ivanter, B. F. Kirillov, B. A. Nikol'skiĭ, A. V. Pirogov, A. N. Ponomarev, V. A. Suetin, V. G. Grebinnik,¹⁾ V. N. Duginov,¹⁾ V. A. Zhukov,¹⁾ A. B. Lazarev,¹⁾ V. G. Ol'shevskii,¹⁾ V. Yu. Pomyakushin,¹⁾ and S. N. Shilov¹⁾

I. V. Kurchatov Institute of Atomic Energy, Moscow

(Submitted 7 May 1991)

Zh. Eksp. Teor. Fiz. **100**, 1353–1357 (October 1991)

The magnetic field experienced by a muon in samarium in its antiferromagnetic state for $T = 16\text{--}105$ K was determined. The results indicated that the muon was localized in an octahedral interstice. The temperature dependence of the magnetic susceptibility associated with the antiferromagnetic ordering at $T_2 = 14$ K was measured in zero external magnetic field. The corresponding paramagnetic temperature was found to be $\Theta = -6.7$ K. The contact magnetic field of the polarized conduction electrons at the muon was determined.

The magnetic properties of samarium were investigated by the neutron-diffraction method¹ and by measuring the magnetization.² The muon method made it possible to obtain additional information on the properties of this complex magnetic material.

Our samarium sample consisted of six disks 30 mm in diameter and 5 mm thick. The disks were initially polycrystalline with $\lesssim 0.0001$ wt.% of metallic impurities and $\lesssim 0.001$ wt.% of gaseous impurities, except for oxygen whose content was $\lesssim 0.01$ wt.%. Subsequent annealing under bidirectional compression in an inert atmosphere increased the dimensions of the single crystals in the disk to 1–5 mm. In the course of the measurements the sample was placed in a special cryostat where it was cooled in a stream of gaseous helium to the prescribed temperature. The temperature of the sample was measured to within $\delta T = 0.1$ K. The experiments were carried out using the phasotron in the Laboratory of Nuclear Problems of the Joint Nuclear Research Institute in Dubna.

Our experiments yielded the time dependence

$$N(t) = N_0 \exp(-t/\tau) [1 + aP(t)] + F \quad (1)$$

of the number of $\mu^+ \rightarrow e^+$ decay positrons escaping along the direction of polarization of muons in zero magnetic field ($H < 0.3$ Oe). Here, $P(t)$ is a function describing the relaxation and precession of the muon spin under the influence of internal magnetic fields B ; $\tau = 2.2 \times 10^{-6}$ s is the muon lifetime; a is the experimental coefficient representing the asymmetry of the angular distribution of the $\mu^+ \rightarrow e^+$ decay positrons; F is the background.

The values of the field B at a muon were determined from the Larmor precession frequency $\omega = \gamma B$ of the muon spin, where γ is the gyromagnetic ratio for the muon. The measured fields B corresponded to interstices in the crystal where the muons were localized. Figure 1 shows the Fourier spectrum

$$n(\omega) = \int P(t) \cos(\omega t) dt \quad (2)$$

with the function $P(t)$ at $T = 30$ K. It is clear from Fig. 1 that muons were localized in a samarium crystal in two magnetically inequivalent interstices where the muon precessed at frequencies $\omega_1 = \gamma B_1$ and $\omega_2 = \gamma B_2$. The two muon precession frequencies were observed throughout the temperature range $T_1 < T < T_2$, where $T_1 = 106$ K and $T_2 = 14$ K are, respectively, the antiferromagnetic ordering tempera-

tures of the hexagonal and cubic layers of the samarium crystal.¹ The temperature dependences of the fields $B_1(T)$ and $B_2(T)$ at $T = 16\text{--}105$ K are plotted in Fig. 2: they demonstrate that the fields B_1 and B_2 were not proportional and the ratio B_1/B_2 increased as a result of cooling. It is also clear from Fig. 2 that cooling saturated the field B_2 and increased the field B_1 .

We can account for the observed relationships by considering the crystal and magnetic structures of samarium. Figure 3 shows a sequence of atomic layers A , B , and C in the rhombohedral lattice of α -samarium oriented at right-angles to the hexagonal axis of the crystal. It is clear from Fig. 3 that the sequence is $ABABCBCACA$. The indices c and h used in Fig. 3 represent the cubic and hexagonal symmetry of the immediate environment of atoms in the layers with these symmetries. The crystal lattice of samarium has two types of interstices between the adjacent layers where the muon can be localized; they are tetrahedral and octahedral. The octahedral interstices are located half-way between the layers and the tetrahedral ones are displaced relative to this average position and are closer to one of the layers between which they are located. Moreover, we shall distinguish hh interstices located between two hexagonal h layers and hc interstices between hexagonal h and cubic c layers.

The antiferromagnetic structure of samarium, which exists in the range $T_2 < T < T_1$, is shown on the right of Fig. 3. In this temperature range the magnetic moments of pairwise distributed hexagonal layers are oriented in parallel along the hexagonal axis of the crystal and the magnetic moments of the adjacent pairs of the hexagonal layers have opposite directions. The arrows show the directions of the magnetization vectors of the hexagonal h layers. The magnetic moments of the cubic layers become antiferromagnetically ordered¹ only in the temperature range $T < T_2$. The symbol 0 on the right-hand side of Fig. 3 denotes the absence of polarization of the atoms in the cubic c layers in the investigated temperature range $T_2 < T < T_1$.

It is clear from Fig. 3 that in the temperature range $T_2 < T < T_1$ the crystal lattice of samarium has two magnetically inequivalent octahedral interstices (hh , hc) and three magnetically inequivalent tetrahedral interstices (one of the hh type and two hc). Two values of the magnetic field B_1 and B_2 at the muon are observed experimentally. It therefore follows that a muon is localized in the octahedral interstices of the samarium crystal.

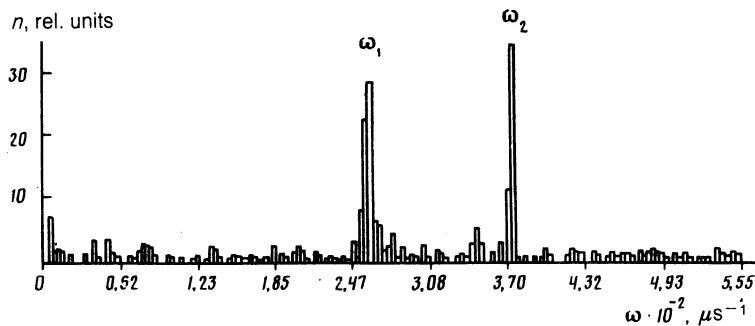


FIG. 1. Fourier spectrum $n(\omega)$ of the function $P(t)$ at $T = 30$ K.

Let us now consider the temperature dependence of the field $B_1(T)$ shown in Fig. 2; this field increases considerably as a result of cooling and is not proportional to the field $B_2(T)$. This behavior of the field B_1 can be explained by the temperature dependence

$$\chi(T) \propto (T - \Theta)^{-1} \quad (3)$$

of the paramagnetic susceptibility $\chi(T)$ of the electron spins in the hc interstices, where the source of magnetization is the dipole field of the nearest hexagonal layers, proportional to B_2 . Here, Θ is the paramagnetic Néel temperature related to the antiferromagnetic ordering of the cubic layers of the crystal lattice of samarium at $T_2 = 14$ K. The characteristic features of the internal magnetizing field should be pointed out: this field acts only on conduction electrons at the hc interstices and it vanishes at the positions of ions in the cubic plane of the crystal. The expression (3) for $\chi(T)$ leads to the following theoretical temperature dependence of the field $B_1^{\text{theor}}(T)$:

$$B_1^{\text{theor}}(T) = \alpha B_2(T) + \alpha B_2(T) \frac{\beta}{T - \Theta} = \alpha B_2(T) \left(1 + \frac{\beta}{T - \Theta} \right), \quad (4)$$

where α and β are numerical constants. Here, the first term determines the contribution made to $B_1^{\text{theor}}(T)$ by the ex-

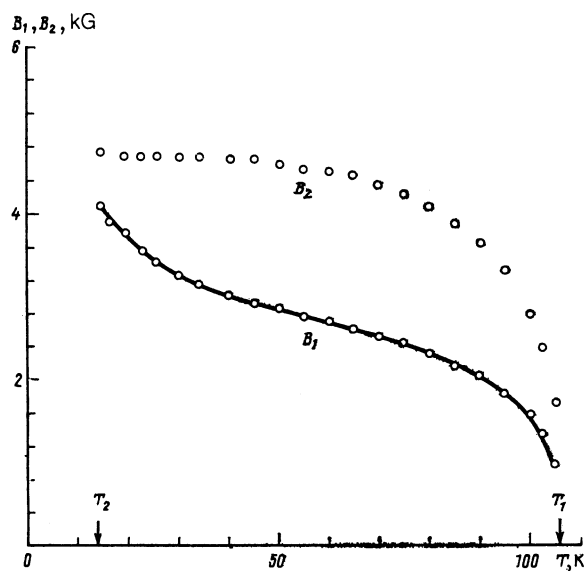


FIG. 2. Experimental dependences $B_1(T)$ and $B_2(T)$ of the magnetic fields at a muon in samarium at $T = 16$ – 105 K. The continuous curve is the theoretical dependence $B_1^{\text{theor}}(T)$ calculated using Eq. (4).

change interactions, whereas the second represents the paramagnetic magnetization of electrons at the interstices. Figure 2 shows $B_1^{\text{theor}}(T)$ calculated from Eq. (4) with the following values of the parameters Θ , α , and β selected by finding the best fit to the data:

Θ , K	α	β , K
-6.7 ± 1.5	0.47 ± 0.01	18 ± 2

The negative value $\Theta < 0$ agrees, as expected, with the antiferromagnetic transition at $T = 14$ K. The good agreement between the experimental $B_1(T)$ and theoretical $B_1^{\text{theor}}(T)$ temperature dependence of the field B_1 is empirical confirmation of the postulated process of paramagnetic magnetization of electrons in the hc interstices. The absence of such magnetization in the hh interstices near the temperature $T_2 = 14$ K can be explained by the weak interaction of these electrons with ions in the cubic plane which becomes ordered at T_2 .

The experimental values of B_1 and B_2 plotted in Fig. 2 should be compared with the dipole fields

$$B_d = \left| \sum_i \frac{-\mathbf{M}_i r_i^2 + 3(\mathbf{M}_i \mathbf{r}_i) \mathbf{r}_i}{r_i^5} \right|,$$

created at a muon at temperatures $T_2 < T < T_1$ by the ordered magnetic moments \mathbf{M}_i of the hexagonal-layer ions in the crystal lattice of samarium. Here, \mathbf{r}_i is the radius vector of the i th ion relative to a muon localized at an octahedral (tetrahedral) interstice; the summation is carried out over all the ions in the crystal. In the calculations we assume

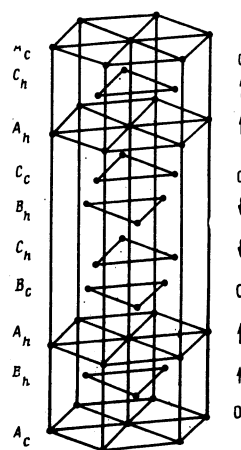


FIG. 3. Crystal magnetic structures of samarium (for explanations see text).

TABLE I. Dipole magnetic fields B_d (in kilogauss) at octahedral and tetrahedral hh and hc interstices in samarium.

Interstice	B_d^{hh}	B_d^{hc}	B_d^{hc}
Octahedral	1,75	0,88	—
Tetrahedral	2,27	1,72	0,60

$M = (5/7)\mu_B$, corresponding to the fully oriented magnetic moment of the ground state ($L = 5, S = 5/2, J = 5/2$) of a trivalent samarium ion and to the values $a = 3.6309 \text{ \AA}$ and $c = 26.035 \text{ \AA}$ of its crystal lattice parameters.³ The values of the dipole fields B_d calculated in this way for the octahedral and tetrahedral hh and hc interstices in samarium are listed in Table I. We recall that the samarium lattice has two inequivalent octahedral and three tetrahedral interstices.

The dipole fields given in Table I are considerably less than the values B_1 and B_2 found experimentally (see Fig. 2). The difference is related to the magnetic field created at a muon by polarized conduction electrons, the majority of which form a contact field $B_c = (8/3)\pi\mu_B\rho(0)P_e$, where $\rho(0)$ is the density of the wave function of electrons at a muon and P_e is the polarization of the conduction electrons. For example, the contact field B_c^{hh} at an octahedral hh interstice at $T = 20 \text{ K}$ can be estimated as follows:

$$B_c^{hh} \approx B_2 - B_d^{hh} = 4,70 - 1,75 = 2,95 \text{ kG.} \quad (5)$$

In the calculation of the approximate value given by Eq. (5) it is assumed that the directions of the fields B_c^{hh} and B_2 coincide. This hypothesis is based on the following consider-

ations. Calculations of the dipole field showed that the fields B_d had octahedral and tetrahedral interstices which are antiparallel to the polarization \mathbf{M} of the atoms in the nearest hexagonal planes. The conduction electrons should be polarized in the same way.

It is clear from the results obtained for B_d that in the case of octahedral interstices the ratio $B_d^{hc}/B_d^{hh} = 0.50$ is close to the experimental value $\alpha = 0.47 \pm 0.01$ given above. This may be regarded as an additional argument in support of the earlier conclusion that the muon is localized at an octahedral interstice in the samarium sublattice.

The authors are grateful to N. E. Zein, M. I. Katsnel'son, and A. V. Trefilov for valuable discussions, and to A. F. Burtsev for his help in this investigation.

¹⁾ Joint Institute of Nuclear Research, Dubna.

¹ W. C. Koehler and R. M. Moon, Phys. Rev. Lett. **29**, 1468 (1972).

² K. A. McEwen, P. F. Touborg, G. J. Cock, and L. W. Roeland, J. Phys. F **4**, 2264 (1974).

³ V. A. Finkel', Structure of Rare-Earth Metals [in Russian], Metallurgiya, Moscow (1978), p. 50.

Translated by A. Tybulewicz